

LEGIBILITY NOTICE

A major purpose of the Technical Information Center is to provide the broadest dissemination possible of information contained in DOE's Research and Development Reports to business, industry, the academic community, and federal, state and local governments.

Although a small portion of this report is not reproducible, it is being made available to expedite the availability of information on the research discussed herein.

LA-UR--88-1015

DE88 007823

TITLE THE ELECTRONIC STRUCTURE OF CONDENSED MOLECULAR SYSTEMS

AUTHOR(S) Richard A. LeSar, T-11

SUBMITTED TO NATA Advanced Study Institute on "Simple Molecular Systems at Very High Densities," Les Houches, France, Mar. 29 - Apr. 5, 1988

DISCLAIMER

This report was prepared as an account of work sponsored by an agency of the United States Government. Neither the United States Government nor any agency thereof, nor any of their employees, makes any warranty, express or implied, or assumes any legal liability or responsibility for the accuracy, completeness, or usefulness of any information, apparatus, product, or process disclosed, or represents that its use would not infringe privately owned rights. Reference herein to any specific commercial product, process, or service by trade name, trademark, manufacturer, or otherwise does not necessarily constitute or imply its endorsement, recommendation, or favoring by the United States Government or any agency thereof. The views and opinions of authors expressed herein do not necessarily state or reflect those of the United States Government or any agency thereof.

By acceptance of this article the publisher recognizes that the U.S. Government retains a nonexclusive, royalty-free license to publish or reproduce the published form of this contribution or to allow others to do so, for U.S. Government purposes.

The Los Alamos National Laboratory requests that the publisher identify this article as work performed under the auspices of the U.S. Department of Energy.

100-1015

Los Alamos National Laboratory

DISTRIBUTION OF THIS DOCUMENT IS UNLIMITED

THE ELECTRONIC STRUCTURE OF CONDENSED MOLECULAR SYSTEMS

Richard LeSar

Los Alamos National Laboratory
Los Alamos, NM 87545

INTRODUCTION

Fundamental to almost all discussions of molecular systems at high densities is the assumption that the system consists of molecular units, with the electrons tightly bound to a specific molecule and whose intermolecular interactions can be described, at least to first order, by a pair potential. Here we present a quick overview of the electronic structure of these insulating systems, with an emphasis on what we know about the changes induced in the molecules as they are compressed to high densities and how those changes may affect the physical and chemical properties of the molecular system.

It is useful to distinguish between classes of insulators based on how the electrons are distributed. In *covalent* crystals, there is considerable electronic density in the interstitial regions, as in a metal, but these interstitial electronic distributions are generally localized in specific preferred directions, forming bonds between the atoms. An example of this type of material is diamond, which has a band gap of 5.5 eV, and whose valence electrons are localized in the four directions of the tetrahedron formed by the nearest neighbor carbon atoms. *Molecular* systems, which include rare-gas solids, are considerably different. Here, the electrons are highly localized about their parent nuclei, with very little electronic density in the interstitial regions. The final class consists of *ionic* systems, which are similar to molecular systems except that the systems consist of charged rather than neutral species. The properties of ionic systems are dominated by electrostatic interactions, which play a much less important role in molecular systems. Of course, these three categories are not precise, and one can have, for instance, "covalent" character between molecules in ionic systems, etc. Here we shall concentrate our discussion on molecular systems, in particular on the rare-gas solids (as prototypes of more complicated systems) and on systems with small molecules.

Much of the interest in molecular insulators at high densities has concerned their transformation to metallic behavior. For the rare-gas systems, metallization is reasonably well understood as occurring through a closure of the band gap.¹ Metallization in molecular systems is more complicated, as there seem to be two paths metallization can take. Either the molecular solid may itself become metallic,² with the core states as molecular ions, or, metallization occurs through dissociation to atoms.³ We shall not discuss metallization in detail here, as it is the focus of another paper in this proceedings.⁴

developed,⁵ it is less so for molecular systems. Experimentally, there are techniques that shed some light on these questions, the most important of which involve measurements of the electronic spectra. There are two types of electronic transitions that can occur; from occupied levels to levels below the conduction band, so-called *exciton* transitions; and transitions to the conduction band.⁶ Measurements of these transition energies tell us something about level shifting and broadening. For molecular systems, we also can measure the vibrational frequency shifts. If there is a softening of a molecular mode, it may indicate that there is a change in bonding, though interpretation of such a softening is not always clear.

Changes in the electronic structure of constituent molecules can play an important role in the physics and chemistry of molecular systems at high pressure. There has been, for instance, a long controversy about the role of many-body forces in determining the equation of state of molecular systems. There is considerable evidence that at high densities, potentials based on the interaction between gas-phase molecules are no longer reliable.⁸ As we shall discuss herein, compression of the molecular electronic density in a high-density solid can seemingly account for a large part of the many-body contributions.⁹ The change in molecular electronic density at high pressures cannot be described by adding 3-body and higher terms; the changes depend on the total crystal symmetry.

In Section II, we shall summarize some of what is known about the electronic structure of rare-gas systems at densities far from metallization. We shall discuss experimental and theoretical results for band gaps, electronic spectra etc. We shall also present a simple method to give the perturbative changes in the ground-state electronic structure of closed-shell systems, as well as the results of calculations with this method on Ar. In Section III, molecular systems will be discussed. We shall limit our discussion to a few linear diatomics, for which some data and theory exist.

ELECTRONIC STRUCTURE OF RARE-GAS SOLIDS

In this section, we review some basic properties of the electronic properties of the rare-gas solids. We do not attempt to give a comprehensive review, since a variety of review articles are available in the literature.⁵⁻⁷ In the first part, we discuss some low pressure experimental and theoretical results for the band gap and exciton energies. In the second part, we discuss an approach to the calculation of the electronic structure of molecular systems that yields molecular electronic densities for crystalline systems as a perturbation of the gas-phase electronic structure.

Experiments and Band-Structure Calculations

We begin our discussion of the rare gases with a prototypical example, argon. In Fig. 1, we present a schematic view of its electronic structure. The upper atomic states of argon are shown on the left of this figure. The 3s and 3p levels are completely occupied, and the lowest unoccupied level is the 4s. We leave off other, higher-energy, unoccupied levels for clarity. The energy to remove an electron from the 3p state to the vacuum is the ionization energy, 15.76 eV.¹⁰ If the argon atoms are then placed in a solid, the levels broaden into bands, as shown schematically in Fig. 1. Band-structure calculations indicate the width of the 3p band is on the order of 1 eV.¹¹ The width of the band indicates that there is overlap between p-orbitals on neighboring atoms, though the bonding in this system is still quite localized. The band gap represents the energy necessary to move an electron from the 3p band to the bottom of the conduction band. This energy⁷ (14.3 eV) is slightly less in argon than the ionization energy, as indicated in Table I and represented in Fig. 1 by the conduction band being below the vacuum level. As we shall discuss hereinafter, it is not unreasonable to associate the localized exciton state with the 4s atomic state. In Table I, we give values for the gas-phase ionization potential,

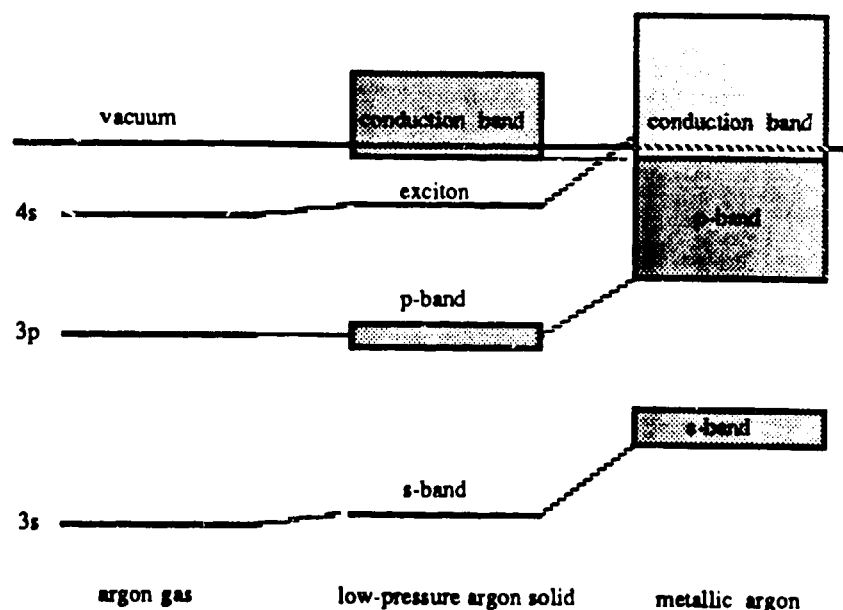


Fig. 1. Schematic view of the electronic structure of argon as discussed in detail in the text. On the left are the atomic levels. In the ground state, these are filled to the $3p$ level. The vacuum represents ionization. In the middle is the band picture of the low-pressure solid and on the right that of the metal.

the band-gap, and the first exciton energy for the rare gases $\text{Ne} \rightarrow \text{Xe}$. At the right of Fig. 1 we show a schematic picture of the band structure of argon metal, as suggested by band-structure calculations. The very narrow bands of the low pressure solid have broadened and shifted until there is overlap of the upper $3p$ band with the conduction band. The metallic transition has been estimated to occur at about 5.8 Mbar.¹

The electronic absorption spectra of the rare-gas solids consist of a series of bands due to exciton transitions and above these a broad spectrum due to band-to-band transitions. There are two limiting cases in the theory of excitons.¹² *Frenkel* excitons are those in which exciton wave function is localized in a small region whose size is roughly that of the nearest neighbor distance. A *Wannier-Mott* exciton, on the other hand, is described as having a weakly interacting electron-hole pair with a large radius relative to the lattice constant. It is perhaps instructive to discuss the Wannier-Mott exciton in more detail. The energy of the exciton transition at the band center is approximately given by⁷

$$E_n = e_g + e_n$$

where e_g is the band gap and e_n is the Coulomb energy of the electron-hole ($e-h$) of the discrete exciton state n . The extent of the exciton wave functions is assumed to be large compared to the lattice constant and the $e-h$ pair is then assumed to not feel the atomic-like nature of the solid, but rather a continuum. The problem then becomes similar to that of a hydrogen atom with the bare Coulomb interaction replaced by $-e^2/\epsilon_d r$, where ϵ_d is the dielectric constant of the medium. Then the $e-h$ energy is given by

$$e_n = -\frac{E_{ex}^b}{n^2} \quad (n=1,2,\dots).$$

E_i	21.50	15.70	14.00	12.15
E_g	21.4	14.3	11.6	9.3
E_x	17.5	12.1	10.2	8.4

^a Experimental values of the ionization potential (E_i ; Reference 10) the band gap (E_g ; Reference 7), and the first exciton energy (E_x ; Reference 13 for Ne, Reference 14 for Ar and Reference 15 for Kr and Xe). All energies are in eV.

where the $e-h$ binding energy and the effective Bohr radius a_B are given by a rescaled H atom:

$$E_{ex}^b = \frac{1}{\epsilon_d^2} \left[\frac{\mu}{m_o} \right] R_H \quad ,$$

and

$$a_B = \epsilon_d \left[\frac{m_o}{\mu} \right] a_H.$$

Here R_H and a_H are the binding energy and Bohr radius for the H atom, respectively, m_o is the free-electron mass, and $\mu^{-1} = m_e^{-1} + m_h^{-1}$ is the reduced mass of the effective masses of the electron and hole. Thus, for Wannier-Mott excitons, where a_B is much greater than the lattice constant, we expect that the series of levels should be hydrogenic and be proportional to $1/n^2$. The picture of a Frenkel exciton, on the other hand, is that of an excited atom at a given lattice site and is applicable only if the exciton wave function is localized in the unit cell about the hole and if it preserves the essential features of the atomic state from which it is derived. We shall not derive the equations for a Frenkel exciton here, but will point out that the procedure is based on finding perturbations to the free-atom wave functions due to long-range dipolar interactions. A plot of the exciton energies versus $1/n^2$ for the rare-gas solids, as illustrated in Fig. 2, indicates that for $n \geq 2$, the excitons can be described as Wannier-Mott type. The $n=1$ excitons, however, seem to be best described as intermediate between the Frenkel and Wannier-Mott pictures.⁵ The $n=1$ exciton energies are fairly close to the atomic transition energies $np \rightarrow (n+1)s$ (Fig. 2). In fact, there is a reasonably close correspondence for all of the excitons to their atomic counterparts in Ne, though for the heavier rare gases that correspondence is less good. It thus seems reasonable to closely associate, at least for $n=1$, exciton transitions in the solid rare gases with the corresponding atomic transitions. If we take that view, then in Fig. 1 we see that the lowest exciton in argon involves the excitation between the occupied $3p$ state and the unoccupied $4s$ state, giving a valence configuration of $3s^2 3p^5 4s^1$. There are two possibilities for that state, a singlet 1P , with the electron spins of the partially occupied orbitals being opposite in sign, and the triplet 3P , with the spins being parallel. The spin-orbit coupling leads to a small energy difference between the two states, as shown in Fig. 2. More detailed descriptions of the exciton states in the rare-gas solids are given elsewhere.^{6,7} It is unfortunate, but because of the large energies associated with these transitions, and because the diamond band edge is between 3 and 5 eV,¹⁶ high-pressure diamond-anvil-cell absorption experiments cannot easily be done on these systems. Only at very high pressures, where the band edge of the transitions drop below that of diamond, are single-photon experiments possible. For example, absorption experiments have been reported for solid xenon, which has the lowest energy transitions, only for pressures above about 30 GPa.¹⁷

The theoretical calculations of the electronic structure of the rare-gas solids have had both successes and failures.^{5,6} In general, all of the modern band-structure methods yield reasonably reliable equations of state (EOS).¹⁸ These techniques generally fail, however, to give values for

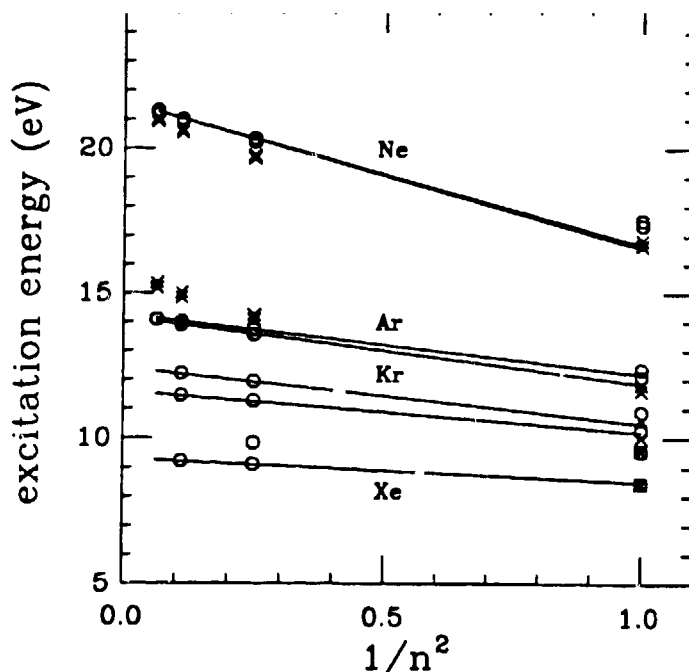


Fig. 2 Experimental electronic excitation energies for the rare gases versus $1/n^2$, as described in the text. The circles are from the solid and the X's are from the gas-phase. The gas-phase data is from Reference 10 and the exciton data is as reported in Table II.

the zero-pressure band gap that are at all close to experiment.^{5,6} For example, estimates of the band gap in argon range from about 8.3 to 18.5 eV, depending on the method.^{11,18} There are a number of problems in calculating excited states associated with the density-functional band-structure techniques, including relaxation effects in the excited state. The most important of these effects, however, seems to be the inadequate treatment of the self-interaction energies, which are larger in the more tightly bound ground states than in the excited, conduction states. Recent advances in treating these self energies may lead to more reliable calculations.¹⁹ There have been a large number of theoretical studies of the excitons in these systems, a review of which is available.⁶

While the band-structure techniques have been successful in determining the electronic energy and (to a certain extent) the excitation spectrum of rare-gas solids, they do not easily yield information that can lead to an improved understanding of the interactions between atoms in a highly condensed solid. A knowledge of these intermolecular interactions, and how they change with density, are necessary if one wants to do dynamical calculations. In the next part of this section we introduce a model that yields the changes in atomic density as a function of pressure, which in turn can be used to examine how the intermolecular interactions change.

The Crystal-Perturbation Model

Most of the theoretical calculations on the electronic structure of the rare-gas solids have started from a band picture. A few years ago, however, we introduced an approximate method to calculate the change in electronic structure of a molecule in a high-density solid from that in the gas phase.⁹ The principle assumptions behind this method were: 1) the electrons in a molecular crystal are tightly bound to their molecular sites; 2) the effects of the crystal environment on the electronic ground- and excited-states can be treated as a perturbation on the free-molecular states. We implement these approximations by performing Hartree-Fock calculations on a molecule in a crystal field calculated with local-density functionals. The advantage to this

crystal wave functions can be used to determine interaction potentials which can be then used in the calculation of crystal properties. A more detailed description of the model is given elsewhere.

We consider the Hamiltonian for a chosen molecule m in a crystal as a sum of the usual gas-phase molecular Hamiltonian H_o and a crystal potential term $V(\vec{r})$, i.e. $H_m = H_o + V(\vec{r})$. The crystal potential is defined as

$$V(\vec{r}) = V_{TFD}[\rho_T] - V_{TFD}[\rho_m], \quad (1)$$

where the Thomas-Fermi-Dirac crystal potential, V_{TFD} , is given by the functional-derivative of the energy of a non-interacting electron-gas, $E[\rho]$,²⁰

$$E[\rho] = \int d\vec{r} \left\{ C_k \rho^{5/3} - C_x \rho^{4/3} + E_c[\rho] + \rho \Phi[\rho] \right\}, \quad (2)$$

which yields,

$$V_{TFD}[\rho] = \frac{5}{3} C_k \rho^{2/3} - \frac{4}{3} C_x \rho^{1/3} + E'_c[\rho] + \Phi. \quad (3)$$

The terms in Eq. (3) represent the kinetic, exchange, correlation, and Coulomb potentials, respectively. The constants $C_k = (3/10)(3\pi^2)^{2/3}$ and $C_x = (3/4)(3/\pi)^{1/3}$ are the usual constants for the non-interacting electron-gas kinetic and exchange density functionals.²⁰ In our applications, we used a correlational potential, E'_c , derived from the correlational-energy functional, E_c , of Gordon and Kim.²² ρ_T in Eq. (1) is the total electronic density of the system given by a sum over the molecules in the system

$$\rho_T(\vec{r}) = \sum_i \rho_i(\vec{r} - \vec{r}_i), \quad (4)$$

where ρ_i is the atomic electronic density of molecule i . ρ_m in Eq. (1) is the density of the chosen molecule. This perturbation term is added to the molecular Hartree-Fock Hamiltonian and the crystal wave function determined with standard Hartree-Fock techniques.

Application of this model to solid fcc argon allows for a great simplification in the calculations. By expanding the crystal potential, $V(\vec{r})$, in the Kubic Harmonics,²³ we see that only the spherically symmetric first term couples to the s and p states of argon. Thus, the perturbation integrals in the Hartree-Fock calculations of the argon wave functions depend only on r . The computational procedure is straightforward. For a given volume, we calculate the crystal potential by evaluating the expressions in Eqs. (1-4) with gas-phase electronic densities for the argon atoms. After determining the spherically-symmetric term in the Kubic Harmonic expansion, we determine a new wave function with a Hartree-Fock calculation that includes the crystal potential. This yields a new atomic wave function, from which, at the same volume, a new crystal potential can be found. This procedure is applied iteratively until convergence is reached (no more than two times), giving the crystal-atomic wave function for that volume. Note that the procedure as described here differs somewhat from that described in our first paper.⁹

The output from the above procedure is the atomic wave function from which one can obtain the perturbed atomic electron density. This electron density can then be used to determine the interactions between the atoms with the use of the Gordon-Kim (GK) electron-gas

$$V_{ij} = E[\rho_i + \rho_j] - E[\rho_i] - E[\rho_j] , \quad (5)$$

where $\mathcal{E}[\rho]$ is the electron-gas energy of Eq. (2), and ρ_i is the electronic density of molecule i . To correct for a variety of problems, such as the exchange self-energy, the electron gas terms in Eq. 2 (kinetic, exchange, and correlation) are multiplied by numerical correction factors that depend only on the number of electrons.²⁴ Short-range potentials calculated with the GK model show very good agreement with experiment, especially when the ease of the calculations is taken into account.^{24,25} Application to uncharged species requires addition of the long-range dispersion terms, which we modify with a damping function at short-range.²⁵ It is also possible to use the GK method to evaluate many-body short-range contributions to the lattice energy.²⁶ Given the converged crystal wave function for a given volume, the lattice energy can then be determined with potentials derived with the GK model. The pressure is then found as $P = -\partial E/\partial V$. Details of the lattice calculations are given elsewhere.⁹

In Fig. 3, we show the mean-square radius ($\langle r^2 \rangle^{1/2}$) as a function of density for solid argon. As is clear from that picture, the extent of the argon atoms in the crystal decreases with increasing density. The driving force for this compression is the reduction in the intermolecular interactions balanced by the gain in the atomic self energy due to increased electron-electron repulsion. Of course, if the size of the constituent atoms decreases, then, at a given pressure, the volume of the system can decrease. This can be clearly seen in Fig. 4, where we have plotted the experimental pressure-volume curve for argon at room temperature²⁷ along with two theoretical curves. The dashed curve was determined at 0 K with a GK potential based on gas-phase argon atomic densities; the solid curve is from similar calculations but with the crystal atomic wave functions. Note that we see a softening of about 2% in the volume at high pressures with the use of the crystal-atomic wave function, bringing the theoretical curve into much better agreement with experiment. Recent work by Barker et al.²⁸ indicates that including this volume

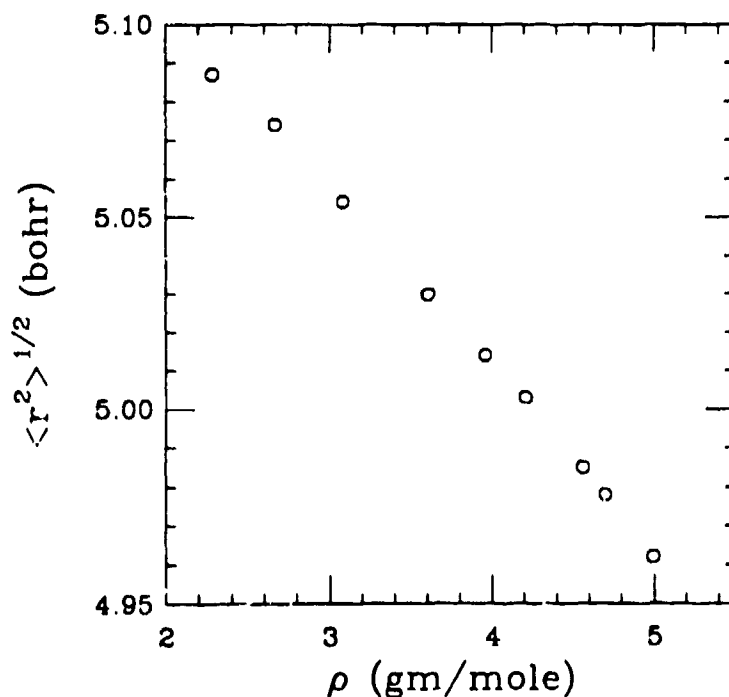


Fig. 3 Mean-square radius of the crystal-atomic wave function as a function of density for solid argon. The pressure range of this figure is about 2 - 80 GPa. The gas-phase value is 5.102 bohr.

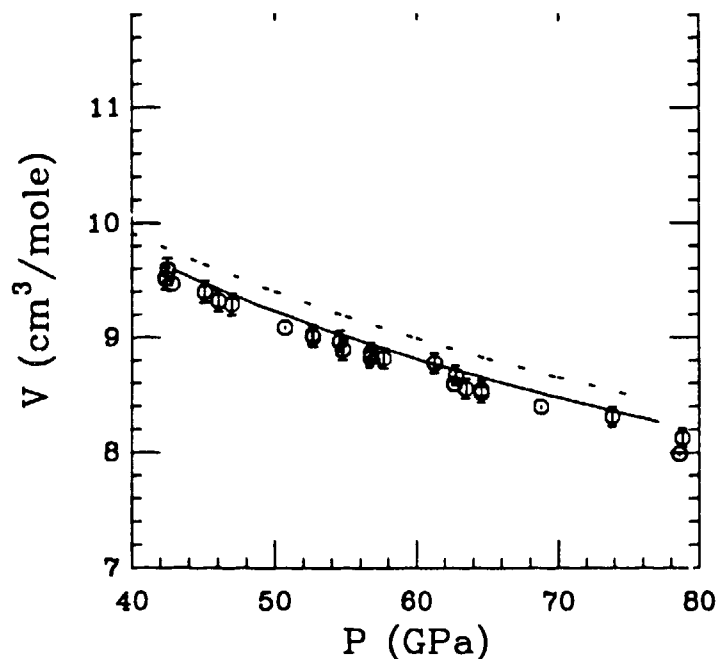


Fig. 4 Volume versus pressure for solid argon. The circles are the experimental values,²⁷ the dashed curve is from a theoretical calculation with a pair potential, and the solid curve incorporates the changes in the crystal-atomic wave function.

correction to the pressure-volume curve calculated with a highly accurate *ab initio* potential leads to quite good agreement with the high-pressure EOS. An analysis of the various many-body contributions to the argon and xenon equations of state is in preparation.²⁹

If we assume that the exciton states are atomic like, then it is also possible to calculate the exciton spectra with this method. As shown in Fig. 5, we get reasonable agreement with the experimental $n=1$ excitons for argon. Much of the error in our calculations probably stems from the use of Hartree-Fock calculations for the atom, since no electron correlation is included. As pressure is increased, we see an increase in the exciton energy due to increased interactions of the more diffuse excited state with the rest of the crystal. We have calculated the mean-square radius of the excited-state wave function and can compare it to the lattice constant. We find that at zero pressure the ratio between the mean square radius of the $4s$ electron wave function and the nearest neighbor distance ($\langle r^2 \rangle^{1/2}/a_{nn}$) is about 0.8 at zero pressure. The corresponding ratio for the ground state wave function is about 0.7. Note that the excited state is still within the first neighbor shell at zero pressure, indicating that a perturbed-atom approach is reasonable. If we assume the radii of the excited-state orbitals scales with n as in Wannier-Mott theory, then for the $n=2$ exciton, $\langle r^2 \rangle^{1/2}/a_{nn} \approx 3.2$, which includes the first nine neighbor shells. By pressures of about 50 GPa, we find that the ratio for the $n=1$ state has increased to about 1.2.

The picture that emerges with this model for changes induced in molecular electronic densities at high densities is a simple one; the atoms and molecules themselves compress to lower their interaction with their neighbors. This idea is not new. It is well known, for instance, that anions in ionic crystals reduce in size due to the electrostatic interactions.²⁶ Early models of atoms at high pressures, namely atoms in hard, spherical boxes,³⁰ showed similar trends, as did a calculation of hydrogen in a spheroidal box.³¹ We should point out that this molecular compression is a true many-body effect; it depends on the full crystal symmetry and cannot be estimated as a sum of 3-body, 4-body etc. terms.

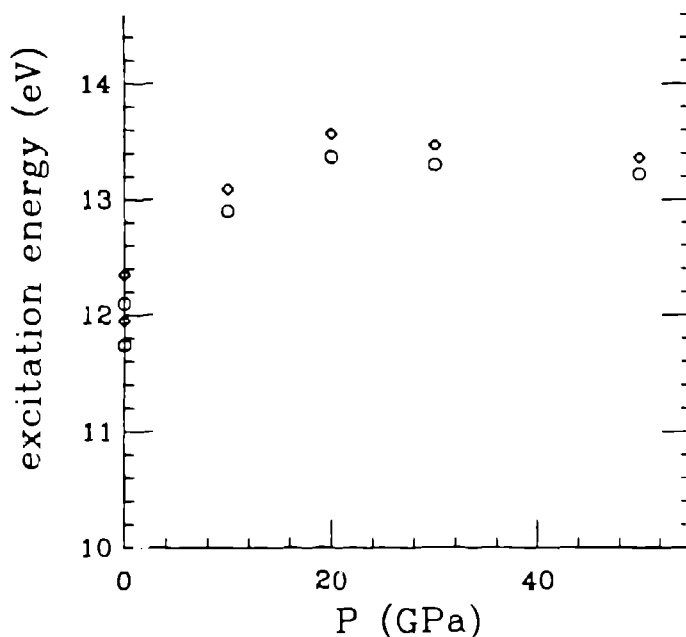


Fig. 5 Calculated exciton transition energies for solid argon. The circles are for the 3P excitons and the diamonds are for the 1P . The filled symbols at zero pressure are the experimental results of Reference 14.

ELECTRONIC STRUCTURE OF MOLECULAR SOLIDS

While our understanding of the electronic structure of rare-gas solids is considerable, we know much less about the electronic properties of condensed molecular systems. In this section, we first review the theoretical approaches that have been taken to calculate the electronic structure of simple molecular crystals. We then shall review some of the experimental data on solid O_2 , I_2 , C_2H_2 , and N_2 , which show different types of changes in electronic structure at high pressures.

Before we go on to discuss molecular solids, let us first review the electronic structure of isolated molecules. In Fig. 6, we show a schematic view of how the molecular orbitals are related to the atomic levels for a simple, first-row, homonuclear diatomic molecule. The atomic $1s$ orbitals are not shown. The $2s$ orbitals hybridize to form bonding and antibonding orbitals, designated in Fig. 6 as 2σ and $2\sigma^*$, respectively. The six atomic $2p$ orbitals (three on each atom) can combine in two ways. One set, pointing along the molecular bond, will form a pair of σ orbitals (3σ and $3\sigma^*$) and the others will form two degenerate sets of orbitals, the 1π and $1\pi^*$ orbitals. The π orbitals arise from the combination of p orbitals lying perpendicular to the bond; the degeneracy arises from the equivalence of the orthogonal directions. Each of these orbitals can have two electrons of opposite spin. From this simple picture, we can understand the relative stability of the diatomic molecules. Each nitrogen atom contributes five valence electrons, giving a total of ten. Adding these electrons to the molecular orbitals gives a $2\sigma^2$, $2\sigma^{*2}$, $3\sigma^2$, and $1\pi^4$ configuration (the numerical superscript indicates the occupancy). The $2\sigma^2$ and $2\sigma^{*2}$ taken together do not add to the binding of the molecules, so N_2 is considered to have a triple bond consisting of a σ and two π bonds. Indeed, nitrogen has the strongest known chemical bond. Oxygen has two additional electrons. These must go into the unfilled $1\pi^*$ orbitals, giving a net bonding of order two, with each π^* electron roughly canceling the binding of a π electron. To minimize Pauli repulsion, the two electrons will have the same spin and therefore must be in different π^* orbitals. Thus, O_2 has a net magnetic moment. F_2 has two more electrons in the $1\pi^*$ orbitals, and thus a bond order of one and a closed-shell configuration. I_2 has

Theoretical Approaches

The calculation of the electronic structure of isolated molecules is a thriving industry,³² and we shall not deal with it here. Suffice it to say that the main problems facing the quantum chemist have to do with the calculation of the electron correlation energy. Standard quantum chemical techniques involve using the Hartree-Fock approach, which has no correlation energy. The addition of configuration interactions lead to better results, but are very complicated and computer intensive.³² Density-functional methods, which use an accurate correlational density functional, have met with some success when applied to molecular systems.³³

There have been relatively few calculations of the electronic structure of molecular solids. One approach has been to use standard quantum chemical techniques to study a cluster of molecules arranged as in a crystal lattice. These studies are limited by edge effects, unless the cluster is quite large.³⁴ Standard density-functional techniques, such as those used to study covalent solids, can be used to study molecular systems. As far as we know, however, only for hydrogen^{3,35} and nitrogen³⁶ have accurate calculations been made with these techniques on the molecular solids. The principle uncertainty in the application of the local-density-functional schemes is the extent to which the local-density approximation describes solids that range from separated, strongly bound molecules to monatomic solids. Because of computational difficulties, the density-functional calculations are probably limited to structures with small numbers of molecules per unit cell. Another approach has been to use Hartree-Fock theory with symmetry-adapted Bloch orbitals to examine the exciton structure.³⁷ Finally, standard quantum chemical procedures have been modified for treating molecular solids. In the method introduced by O'Shea and Santry,³⁸ a perturbation expansion is developed in which the isolated molecule corresponds to the zeroth-order term and the intermolecular interactions are included as higher order perturbations. Their techniques have been applied to solid HF and HCl by Anderson and Santry,³⁹ where the change in molecular dipole and quadrupole moments in the solid were studied. They found roughly a 20% change in those quantities. Their method, being a perturbation

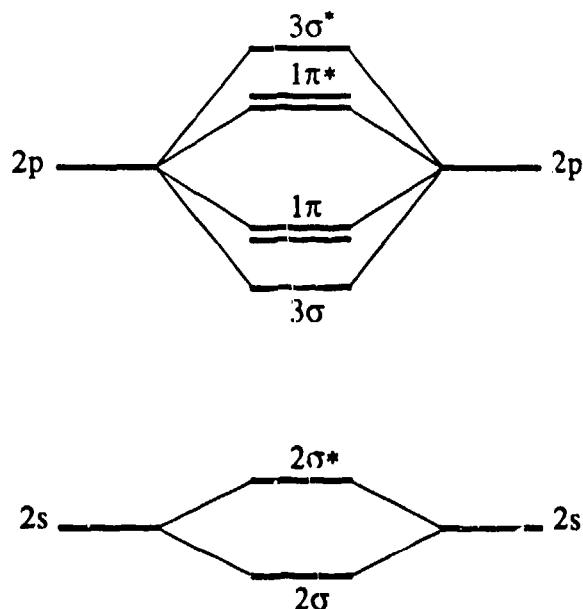


Fig. 6 Schematic diagram of the valence molecular orbitals for a second-row, homonuclear, diatomic molecule. The closely-spaced lines for the π states indicate that they are degenerate.

that does not depend on a perturbation expansion and includes all many-body interactions. The system is divided into subcells and the crystal molecular orbital is made up of orthonormalized subcell orbitals. The total crystal energy can then be partitioned into the subcell contributions. The subcell energy is written as a lattice sum over terms that depend on the intercell overlap integrals. Her method seems to be computationally quick, at least for limited basis sets. She has applied⁴¹ her technique to solid molecular hydrogen and finds good agreement with experimental and theoretical PV curves at very high densities. Her approach, as now developed, does not include any correlational effects nor is applicable to open-shelled systems.

Solid O₂ at High Pressures.

As noted above, the unpaired, spin-aligned electrons in molecular O₂ lead to a magnetic moment, which has important ramifications to the solid phase diagram.⁴² The low-temperature α phase, for example, owes its stability over the rhombohedral β structure to its antiferromagnetic order.⁴³ The orthorhombic δ structure also seems to be stabilized in part by magnetic ordering.⁴⁴ Finally, there is evidence that strongly suggests that significant *intermolecular* covalent bonding has developed between the $1\pi^*$ orbitals on neighboring molecules in the high-pressure ϵ structure.⁴⁵ Here, we shall concentrate on the evidence for intermolecular bonding.

At room temperature and near 10 GPa, there are three solid structures in O₂,⁴⁶ each of which is colored. Near 9.6 GPa, the β structure transforms to the δ structure, which in turn transforms to ϵ around 10 GPa. The transformation to the ϵ structure is accompanied with the beginnings of a very intense infrared signal from the O₂ intramolecular vibration.⁴⁵ The structures of the β and δ phases have been determined,⁴⁸ and they share features in common; they consist of planes of O₂ molecules with the molecules aligned perpendicular to the planes. Analysis of powder x-ray work⁴⁸ suggests that that planar structure is maintained in the higher-pressure ϵ structure. The anisotropies in the optical spectra are consistent with this model. The

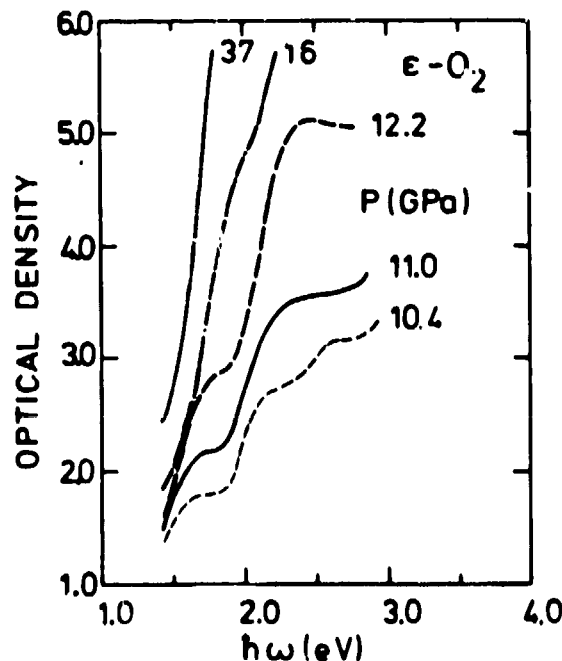


Fig. 7 Absorption spectra perpendicular to the O₂ planes in ϵ -O₂, from Ref. 46.

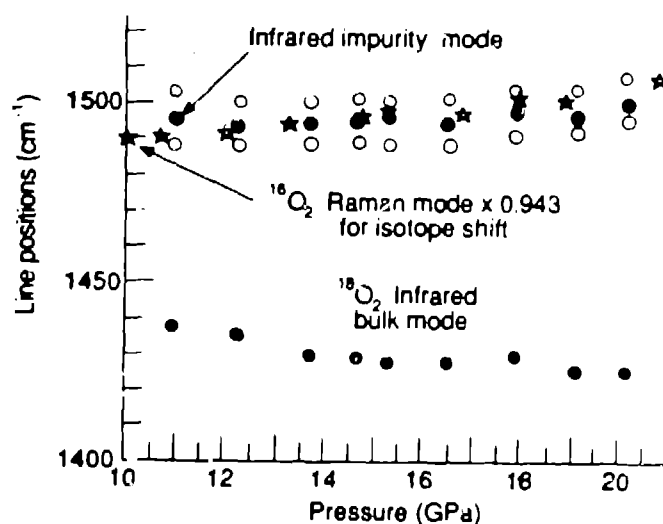


Fig. 8 Pressure dependence of Raman (○) and infrared (●) features for 6% $^{16}\text{O}^{18}\text{O}$ in $^{18}\text{O}_2$. Also shown (*) are the data for the single Raman band in $^{16}\text{O}_2$, scaled by the expected isotope shift. From Ref. 45.

colors in O_2 are in contrast to other light diatomic molecules, such as nitrogen, which are transparent in the visible and ultraviolet at similar pressures. Thus O_2 presents a good test case for studying how electronic states are perturbed at high pressures. To that end, Nicol and Syassen reported ⁴⁷ optical-absorption data for solid O_2 in the range of 1.5-3.5 eV over a pressure range up to 40 GPa. In Fig. 7 we show the absorption spectra for light propagating perpendicular to the O_2 planes in the ϵ structure. These are dominated by a band that moves from the uv through the visible with increasing pressure. Nicol and Syassen assign this band to a transition from a $1\pi^4 1\pi^{*2}$ configuration to a $1\pi^3 1\pi^{*3}$ configuration, the latter of which is mixed with charge-transfer states.

In Fig. 8 we show recent infrared and Raman data by Agnew et al.⁴⁵ of the O_2 stretching frequency in the ϵ phase for a series of isotopic mixtures. The data shows a number of interesting features, including a doubling of the Raman band in $^{16}\text{O}_2$ due to $^{16}\text{O}^{18}\text{O}$ impurities. The pressure-dependence of the infrared and Raman signals show opposite behavior; the Raman signal shifts to higher frequency and the infrared to lower. The infrared impurity signal, however, tracks very well with the Raman shift. They analyzed this data in terms of a model that incorporates a pairwise interaction between nearest neighbor molecules within the O_2 planes. They could account for the frequency shifts and intensities with this simple model, and were led to the conclusion that very strong anisotropic intraplanar interactions lead to chains of oxygen pairs. The decrease in the infrared frequencies was attributed to a weakening of the O_2 bond. One interpretation that fits explains both the large increase in intermolecular interactions and the bond weakening is that there is a beginning of covalent bonding between oxygen molecules, through the overlap of the half-filled $1\pi^*$ orbitals. The advent of such bonding seems to be consistent with the optical-absorption data.

Solid I_2 at High Pressures.

The measurement of optical-absorption bands with pressure provides information only about the relative spacing of the energy levels. Thus, our knowledge about details of the ground-state electronic structure is only inferred. Other measurements, such as infrared and

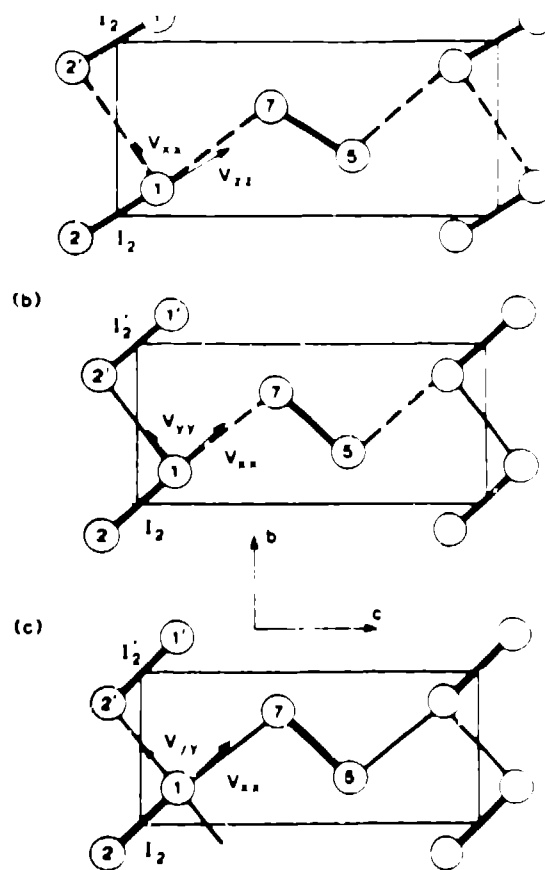


Fig. 9 Schematic representation of the proposed ⁵³ steps in the deformation of iodine. (a) The molecular phase. (b) The I₂-I₂ zigzag chain for 15 ≤ P ≤ 24. This shows quasi one-dimensional behavior. (c) The two-dimensional high-pressure structure.

Raman spectroscopy, also do not give direct information about the local molecular charge distributions. As far as we know, the only experimental technique that will yield such information is Mössbauer spectroscopy,⁵⁰ in which the energy levels of a nucleus are measured. Since these nuclear levels are influenced by their local environment, information about the symmetry of that environment and the local electronic structure can be obtained. Unfortunately, relatively few elements have isotopes that have the low-lying excited states necessary for Mössbauer spectroscopy. Of the simple molecular systems, only I₂ can be studied with this technique. (Other molecular solids, such as SnI₄, can also be studied with Mössbauer techniques.⁵¹) However, iodine is of considerable interest, mostly because it undergoes a metallic transition at relatively low pressure.⁵² Since Mössbauer spectroscopy probes the electronic structure, it can play an important role in our understanding of the molecular insulator-metal transition. Here, we shall briefly review the structural and conductivity data for solid I₂, and then shall discuss those results in light of recent Mössbauer studies.

Before we discuss iodine, however, let us first review some aspects of Mössbauer spectroscopy.⁵⁰ Gamma rays emitted when radioactive nuclei in excited states decay can excite other stable nuclei of the same species. In general, however, this resonant process cannot be observed due to the nuclear recoil, except when the nuclei are fixed within a lattice in a solid and the nuclear recoil energy is less than any lattice modes. The probability of such a recoil-free event depends on the energy of the nuclear gamma ray and so the Mössbauer effect is restricted to certain isotopes with low-lying excited states. In Mössbauer spectroscopy, a Mössbauer nucleus in an excited state decays, and the nuclear levels are determined by detecting the absorption of the

tum quantum number $I > 1/2$, then the nucleus has a quadrupole moment. This nuclear quadrupole moment can couple with the electric field of the surrounding charge distribution, which can lead to a splitting of the Mössbauer spectrum. Since the nuclear quadrupole moment is fixed, the quadrupole splitting reflects the symmetry of the environment and the local electronic structure. For instance for I_2 , the Hamiltonian governing the quadrupole interaction in the ground ($I = 7/2$) and excited ($I^* = 5/2$) states can be written in terms of the principle axis of the electric-field gradient V_{zz} , the asymmetry parameter of the electric-field gradient $\eta = (V_{xx} - V_{yy})/V_{zz}$, and the nuclear quadrupole moment eQ as

$$H = \frac{eQV_{zz}}{4I(I-1)} \left[3I_z^2 - I^2 + \frac{1}{2}\eta(I_+^2 + I_-^2) \right], \quad (6)$$

where I_z^2 , I_+^2 , and I_-^2 are spin operators.⁵³ The experimental Mössbauer spectra can be fit with this form and the quadrupole coupling constant eQV_{zz} and the asymmetry parameter η can be determined.

Solid iodine (Fig. 9) has an optical gap of about 1.35 eV at ambient pressures and becomes metallic at about 16 GPa.⁵² A series of x-ray studies,^{54,55} indicate that there is no structural transition at metallization, i.e. iodine becomes a molecular metal. A transition from the orthorhombic molecular phase to a body-centered orthorhombic monatomic lattice is reported from x-ray studies at about 21 GPa.⁵⁵ Recent x-ray studies report two transitions in the monatomic-metallic state, from the body-centered orthorhombic to a tetragonal lattice at about 45 GPa⁵⁶ and from the tetragonal to a face-centered cubic at about 55 GPa.⁵⁷ However, Raman experiments⁵⁸ did not show conclusively the disappearance of the intramolecular stretching frequency at pressures to 21 GPa, though they did notice an unusually flat relationship between vibrational frequency and pressure. Thus, the Raman data and the interpretation of the x-ray data seem to be contradictory. The Raman experiments to 20 GPa could be explained by a phenomenological model based on molecular iodine that included intermolecular charge transfer terms.⁵⁹

Recent Mössbauer studies shed some light on the issue of the molecular versus atomic character.⁵³ Analysis of the quadrupole coupling constant and the asymmetry parameter of the electric field gradient suggests that there is a change in electronic structure at the metallization pressure (≈ 16 GPa) that involves the formation of zig-zag I_2 chains (Fig. 9b), along which conduction occurs. X-ray data⁵⁵ for the r_{12} and r_{17} distances in Fig. 9b is consistent with this picture. The Mössbauer studies also see a change at about 24 GPa that seems to be the quasi two-dimensional behavior shown in Fig. 9c. However, the evidence indicates that I_2 is the basic structural unit at least up to 30 GPa, which seems to contradict the x-ray studies. It is not possible to definitively reconcile the Mössbauer with the x-ray results. It may have to do with the temperature of the phase line; the Mössbauer work was done at low temperatures (4 K) and the x-ray work at room temperature.

Solid C_2H_2 at High Pressures.

So far we have seen two types of changes in the electronic structure of π molecular systems at high densities. In solid O_2 , the experimental data suggests that there may be the beginning of covalent bonding between the molecules. Solid iodine becomes a molecular metal. In this section, we shall discuss a system that undergoes a high-pressure polymerization reaction; solid acetylene, C_2H_2 .

At ambient pressures, acetylene has two solid forms.⁶⁰ Below about 133 K it is orthorhombic with space group $Cmca$ and is isomorphous with solid molecular iodine. At higher

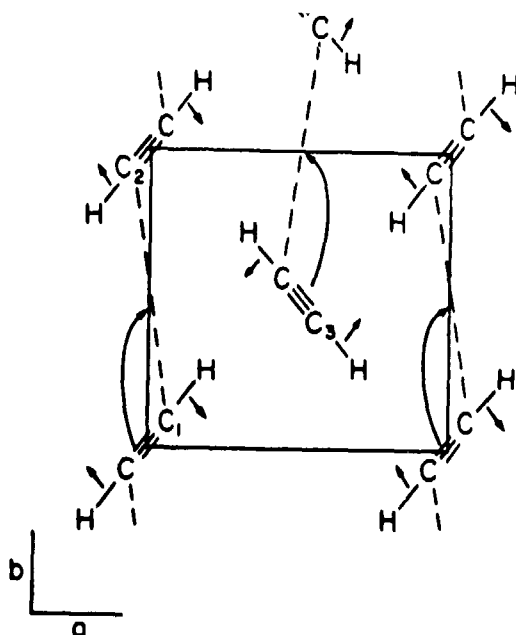


Fig. 10 Structure of the a - b plane of the low-temperature $Cmca$ structure of acetylene.⁶¹ The three-dimensional structure is obtained by stacking such planes at $c/2$, offset by $b/2$. The dashed lines indicate the path originally suggested for polymerization.⁶¹ Experiments suggest,⁶³ however, that polymerization occurs in the b - c plane.

temperatures, it has the $Pa3$ structure. Recently, we suggested⁶¹ that because of the similarities between the structure of solid acetylene and the diacetylenes, acetylene might be expected to polymerize at high pressures with the same topochemical (i.e. no change in symmetry) mechanism as the diacetylenes. The path we suggested is shown in Fig. 10. Our calculations, which were at 0 K, involved the use of the Gordon-Kim model to determine the structure of the orthorhombic phase as a function of pressure, and simple bond-length arguments to predict polymerization paths. Using a rule of thumb from the diacetylenes that reaction occurs when the $C-C$ distance drops below 4 Å, we showed that the r_{12} distance in Fig. 10 was not the nearest intermolecular $C-C$ distance and that we would not expect the reaction to occur cleanly in the $a-b$ plane. The nearest neighbor carbons were in fact along the $b-c$ plane. We suggested that a highly crosslinked product would be the likely reaction product. Subsequent to our calculations, Aoki et al.⁶² reported the observation of a polymerization from the orthorhombic phase at 3.5 GPa which is accompanied with a color change from clear to deep ruby red. Further experimental work⁶³ suggests that the reaction did not occur in the $a-b$ plane, but rather along the diagonal in the $b-c$ plane (perpendicular to the paper in Fig. 10). If we examine the calculated structure,⁶¹ we see that indeed the nearest neighbor C atoms are involved in the reaction. It is interesting to note that that distance is about 3.6 Å at zero pressure and zero temperature and has reduced to about 3.0 Å at 4 GPa.

The polymerization of acetylene provides a relatively straightforward example of an important class of chemical reactions at high pressures. There are a number of advantages in the study of acetylene polymerization rather than, for example, CO, which is known to polymerize at about 5 GPa.⁶⁴ For one thing, acetylene forms an ordered solid, as opposed to the plastic crystal structure of CO, making the analysis of the reaction mechanism easier. More importantly, we know much about polyacetylene, and do not know the structure of polycarbonmonoxide. Thus, study of the details of acetylene should provide much insight into the general properties of

Solid N₂ at High Pressures.

Our last example of the effects of pressure on molecular electronic structures is solid nitrogen, which is probably the most studied of all molecular systems largely because it is chemically inert. However, recent shock-wave experiments⁶⁵ and theoretical calculations^{36,66} indicate that nitrogen may dissociate at relatively low pressures. Indeed, the theoretical calculations suggest that the dissociation pressure may be less than 100 GPa. However, experimental Raman data shows strong peaks associated with the intramolecular stretch to over 130 GPa.⁶⁷ The Raman vibron peaks split into a number of lines as pressure is increased, indicating a phase transition. The lowest frequency vibron levels off with increasing pressure and then begins to decrease. It is unlikely, however, that this turn down in frequency shift due to electronic structure changes in the material.⁶⁸ Thus, either the theory (admittedly uncertain) is in error or there is a large kinetic barrier to dissociation. The first study of this system that predicted a pressure dissociation compared the energies of a monatomic lattice calculated with band-structure theory to those of the molecular phase calculated with the Gordon-Kim model described earlier and found a transition at about 80 GPa to a simple-cubic monatomic lattice.⁶⁶ Because of restrictions in the band-structure methods used complicated structures could not be studied, however, it was suggested that a three-fold coordinated, arsenic-like, structure might be stable at lower pressures than simple cubic. The subsequent work of Martin and Needs,³⁶ improved upon the early calculations by using the local-density functional method for both the molecular and metallic phases, and considered a number of distorted structures. Analysis of their results showed a barrier of about 1 eV/atom (≈ 12000 K/atom) along the path they considered, with the minimum energy configuration a distorted arsenic-like structure. Because of restrictions in their method, they could not examine solid N₂ in detail in a known nitrogen crystal structure, but had to use the structure of β oxygen. Remarkably, however, they found a transition at essentially the same pressure (70 GPa) as the earlier work. A nice feature of their work is that they could monitor the electronic density changes in a number of intermediate structures from the molecular to the semimetallic arsenic-like phase. While there is uncertainty in the calculations which makes definitive conclusions impossible, the high barrier to reaction (1 eV) can account for the dissociation not being observed at room temperature.

SUMMARY

We have reviewed some of the basic properties of the electronic structure of condensed molecular systems. For the rare-gas solids, we concentrated our discussion on changes in the ground- and excited-state crystal-atomic wave functions as calculated with an approximate theoretical method. Compression of these wave functions leads to a softening of the equation of state at high densities, which seems to account for much of the total many-body effects. This compression is a true many-body effect and cannot be easily decomposable into a sum of 3-body and higher terms.

We reviewed the electronic properties of four molecular systems, each manifesting different behavior at high densities. Because of a general lack of theory of the electronic structure of molecular solids, we restricted ourselves to a descriptive account. Solid oxygen, for instance, seems to exhibit the beginnings of covalent bonding between the π^* orbitals on adjacent molecules in its ϵ phase. It was a combination of optical-absorption data and infrared and Raman spectroscopy that led to these conclusions. Iodine is unique in that it becomes metallic as a molecular crystal at pressures easily obtainable experimentally. It is interesting that the x-ray data, which indicates a transition to a monatomic lattice at 21 GPa, and the Mössbauer spectra, which implies that molecular character is retained to 30 GPa, are in such disagreement. The next system discussed, solid acetylene, is a nice example of high-pressure polymerization and study of this system should shed light on the polymerization of more complicated systems. Finally, we briefly discussed the predicted dissociation of solid molecular nitrogen at high

molecular systems, it would be nice to reconcile the contradictory results.

Molecular systems show a very diverse range of behavior in their electronic structures at high pressures, from metallization to chemistry. As of now, theory is lagging very far behind experiments in providing detailed clues to that behavior. The development of better methods for calculating electronic structures is an important and challenging problem.

ACKNOWLEDGEMENTS

We would like to thank Dean Taylor of the Los Alamos National Laboratory and Malcolm Nicol of UCLA for helpful discussions, and K. Aoki of the National Chemical Laboratory for Industry in Japan for letting me discuss results of his work on the polymerization of acetylene prior to publication. My work was performed under the auspices of the United States Department of Energy and was supported in part by the Division of Materials Science of the Office of Basic Energy Sciences of the Department of Energy.

REFERENCES

1. M. Ross and A. K. McMahan, Metallization of some simple systems, in "Physics of Solids under High Pressure," J. S. Schilling and R. N. Shelton, eds., North Holland Publishing Company, Amsterdam (1981).
2. A. K. McMahan, B. L. Hord, and M. Ross, Experimental and theoretical study of metallic iodine, *Phys. Rev. B* 15:726 (1977).
3. D. M. Wood and N. W. Ashcroft, Structure and screening in molecular and metallic hydrogen at high pressure, *Phys. Rev. B* 25:2532 (1982).
4. M. Ross, Metallization of simple molecules, this volume.
5. For a review of work done prior to 1976: U. Rössler, Band structure and excitons, in "Rare Gas Solids," M. L. Klein and J. A. Venables, eds., Academic Press, London (1976).
6. For a comprehensive treatment of electronic excitations in rare-gas solids: N. Schwentner, E.-E. Koch, and J. Jortner, "Electronic Excitations in Condensed Rare Gases," Springer Tracts in Modern Physics 107, Springer-Verlag, Berlin (1985).
7. M. Ueta, H. Kanzaki, K. Kobayashi, Y. Toyozawa, and E. Hanamura, "Excitonic Processes in Solids," Springer Series in Solid State Sciences 60, Springer-Verlag, Berlin (1986).
8. See, for example: J. A. Barker, Many-body interactions in rare gases, *Mol. Phys.* 57:755 (1986).
9. R. LeSar, Ground- and excited-state properties of solid argon under pressure, *Phys. Rev. B* 28:6812 (1983).
10. C. E. Moore, "Atomic Energy Tables," National Bureau of Standards Circ. 467, National Bureau of Standards, Washington (1949).
11. For example: L. F. Mattheis, Energy bands for solid argon, *Phys. Rev.* 5:A1399 (1964); L. Dagens and F. Perrot, Hartree-Fock band structure and optical gap in solid neon and argon, *Phys. Rev. B* 5:641 (1972); S. B. Trickey, F. W. Averill, F. R. Green, Self-consistent one-electron calculation of the zero-temperature cohesive properties of solid argon, *Phys. Lett.* 41A:385 (1972); S. B. Trickey and J. P. Worth, Electrons and phonons in rare gas crystals: Numerical studies of simple local density models, *Int. J. Quantum Chem. Symp.* 11: 529 (1977); D. Brust, M. Ross, and K. Johnson, The nonmetal to metal transition of Ar and Xe: A combined APW and pseudopotential study, *J. Nonmetals* 1:47 (1972).

13. V. G. Barak, PAIR AND MANY-BODY FORCES IN SOLID ARGON, Phys. Rev. B 20:784 (1979).
14. R. Haensel, G. Keitel, E. E. Koch, M. Skibowski, and P. Schreiber, Reflection spectrum of solid argon in the vacuum ultraviolet, Phys. Rev. Lett. 23:1160 (1969).
15. R. Haensel, G. Keitel, E. E. Koch, M. Skibowski, and P. Schreiber, Reflection spectrum of solid krypton and xenon in the vacuum ultraviolet, Optics Commun. 2:59 (1970).
16. K. Asaumi and Y. Kondo, Effect of very high pressure on the optical absorption spectra in CsI, Solid State Commun. 40:715 (1981).
17. K. Asaumi, T. Mori, and Y. Kondo, Effect of very high pressure on the optical absorption edge in solid Xe and its implication for metallization, Phys. Rev. Lett. 49:837 (1982).
18. For example: A. K. McMahan, Structural transition and metallization in compressed solid argon, Phys. Rev. B 33:5344 (1986); M. Ross and A. K. McMahan, Condensed xenon at high pressure, Phys. Rev. B 21:1658 (1980).
19. J. P. Perdew and A. Zunger, Self-interaction correction to density-functional approximations for many-electron systems, Phys. Rev. B 23:5048 (1981).
20. J. C. Slater, "Quantum Theory of Atomic Structure," Vol. II, Appendix 22, McGraw-Hill, New York (1960).
21. R. G. Gordon and Y. S. Kim, Theory for forces between closed-shell atoms and molecules, J. Chem. Phys. 56:3122 (1972).
22. F. C. von der Lage and H. A. Bethe, A method for obtaining electronic eigenfunctions and eigenvalues in solids with an application to sodium, Phys. Rev. 71:612 (1947).
23. Y. S. Kim and R. G. Gordon, Study of the electron gas approximation, J. Chem. Phys. 60:1842 (1974).
24. M. Waldman and R. G. Gordon, Scaled electron gas approximation for intermolecular forces, J. Chem. Phys. 71:1325 (1979).
25. R. LeSar, Electron-gas plus damped-dispersion model for intermolecular forces: The rare gas and H₂-He, H₂-Ne, and H₂-Ar potentials, J. Phys. Chem. 88:4272 (1984).
26. C. Muhlhausen and R. G. Gordon, Density-functional theory for the energy of crystals: Test of the ionic model, Phys. Rev. B 24:2147 (1981); R. LeSar and R. G. Gordon, Electron-gas model for molecular crystals. Application to the alkali and alkaline-earth hydroxides, Phys. Rev. B 25:7221 (1982).
27. L. W. Finger, R. M. Hazen, G. Zou, H. K. Mao, and P. M. Bell, Structure and compression of crystalline argon and neon at high pressure and room temperature, Appl. Phys. Lett. 39:892 (1981); J. Xu, H. K. Mao, and P. M. Bell, Position-sensitive x-ray diffraction: hydrostatic compressibility of argon, tantalum, and copper to 769 kbar, High Temp.-High Pressures 16:495 (1984). A. P. Jephcoat, "Hydrostatic compression studies on iron and pyrite to high pressures: The composition of the Earth's core and the equation of state of solid argon," The Johns Hopkins University, Baltimore (1985).
28. J. A. Barker, private communication.
29. A. P. Jephcoat, R. J. Hemley, and R. LeSar, Equation of state of solid argon and xenon at high pressure: Theoretical study of pair and many-body forces, in preparation.
30. For example: S. R. de Groot and C. A. ten Seldam, On the energy levels of a model of the compressed hydrogen atom, Physica 12:669 (1946); E. Ley-Koo and Sergio Rubinstein, The hydrogen atom within spherical boxes with penetrable walls, J. Chem. Phys. 71:351 (1979).
31. R. LeSar and D. R. Herschbach, Electronic and vibrational properties of molecules at high pressures. Hydrogen molecule in a rigid spheroidal box, J. Phys. Chem. 85:2798 (1981);
32. A. Szabo and N. S. Ostlund, "Modern Quantum Chemistry: Introduction to Advanced Electronic Structure Theory," Macmillan Publishing Co., New York (1982).
33. O. Gunnarson, J. Harris, and R. O. Jones, Density-functional theory and molecular bonding. I. First-row diatomic molecules, J. Chem. Phys. 67:3970 (1977); O. Gunnarson and R.

C. Jones, Density-functional calculations for atoms, molecules and clusters, *Physica Scripta* 21:394 (1980).

34. See, for example: W. H. Fink, A. Banarjee, and J. Simons, *J. Chem. Phys.* 79:6104 (1983).
35. S. Chakravarty, J. H. Rose, D. Wood, and N. W. Ashcroft, Theory of dense hydrogen, *Phys. Rev. B* 24:1624 (1981); For a Hartree-Fock calculation of the bands see: P. Gianozzi and S. Baroni, Hartree-Fock energy bands in molecular crystals: Solid hydrogen in the cubic phase, *Phys. Rev. B* 30:7187 (1984).
36. R. M. Martin and R. J. Needs, Theoretical study of the molecular to non-molecular transformation of nitrogen at high pressures, *Phys. Rev. B* 34:5082 (1986).
37. A. B. Kunz, Theory of the electronic structure and optical properties of organic solids: Collective effects, in "Quantum Chemistry of Polymers - Solid State Aspects," J. Ladik et al., eds., D. Reidel Publishing Co. (1984).
38. S. F. O'Shea and D. P. Santry, Non-empirical molecular orbital theory of the electronic structure of molecular crystals, *Theoret. Chim. Acta* 37:1 (1975).
39. S. G. Anderson and D. P. Santry, Nonempirical molecular orbital calculations for hydrogen bonded molecular solids: Molecular dipole and quadrupole moments for solid HF and HCl, *J. Chem. Phys.* 74:1780 (1981).
40. S. Raynor, Novel *ab initio* self-consistent-field approach to molecular solids under pressure. I. Theory, *J. Chem. Phys.* 87:2790 (1987).
41. S. Raynor, Novel *ab initio* self-consistent-field approach to molecular solids under pressure. II. Solid H₂ under high pressure, *J. Chem. Phys.* 87:2795 (1987).
42. R. D. Etters, Phase diagram of diatomic molecular solids, this volume.
43. R. LeSar and R. D. Etters, On the character of the α - β phase transition in solid oxygen, *Phys. Rev. B* (in press).
44. R. LeSar and R. D. Etters, unpublished results
45. S. F. Agnew, B. I. Swanson, and L. H. Jones, Extended interactions in the ϵ phase of oxygen, *J. Chem. Phys.* 86:5239 (1987).
46. M. Nicol and K. Syassen, High-pressure optical spectra of condensed oxygen, *Phys. Rev. B* 28:1201 (1983); K. Syassen and M. Nicol, Solid O₂ near 298 K: Raman and electronic spectra of β and ϵ -O₂, in "Physics of Solids under High Pressure," J. S. Schilling and R. N. Shelton, eds., North Holland Publishing Company, Amsterdam (1981).
47. M. Nicol, K. R. Hirsch, and W. B. Holzapfel, *Chem. Phys. Lett.* 68:49 (1979).
48. H. d'Amour, W. B. Holzapfel, and M. Nicol, *J. Phys. Chem.* 85:131 (1981); D. Schiferl, D. T. Cromer, and R. L. Mills, Structure of 'orange' ¹⁸O₂ at 9.6 GPa and 297 K, *Acta Cryst. B* 39:153 (1983).
49. B. Olinger, R. L. Mills, and R. B. Roof, Structure and transitions in solid O₂ to 13 GPa at 298 K by x-ray diffraction, *J. Chem. Phys.* 81:5068 (1984).
50. D. P. E. Dickson and F. J. Berry, Principles of Mössbauer spectroscopy, in "Mössbauer Spectroscopy," D. P. E. Dickson and F. J. Berry, eds., Cambridge University Press, Cambridge (1986).
51. M. Pasternak and R. D. Taylor, Structural and valence properties of the amorphous-metallic high pressure phase of SnI₄, *Phys. Rev. B* (in press).
52. A. S. Balchan and H. G. Drickamer, *J. Chem. Phys.* 34:1948 (1961); B. M. Riggleman and H. G. Drickamer, *J. Chem. Phys.* 38:2721 (1963).
53. M. Pasternak, J. N. Farrell, and R. D. Taylor, Metallization and structural transformation of iodine under pressure: A microscopic view, *Phys. Rev. Lett.* 58:575 (1987); M. Pasternak, J. N. Farrell, and R. D. Taylor, The isomer shift of elemental iodine under high pressure, *Solid State Commun.* 61:409 (1987).
54. O. Shimomura, K. Takemura, Y. Fujii, S. Minomura, M. Mori, Y. Noda, and Y. Yamada, Structure analysis of high-pressure metallic state of iodine, *Phys. Rev. B* 18:715 (1978).

56. Y. Fujii, K. Hase, Y. Ohishi, N. Hamaya, and A. Onodera, Pressure-induced monatomic tetragonal phase of metallic iodine, Solid State Commun. 59:85 (1986).
57. Y. Fujii, K. Hase, N. Hamaya, Y. Ohishi, A. Onodera, O. Shimomura, and K. Takemura, Pressure-induced face-centered cubic phase of monatomic metallic iodine,
58. O. Shimomura, K. Takemura, and K. Aoki, in "Proceedings of the 8th ATRAPT International Conference, Uppsala, Sweden, 1981," C. M. Blackman, T. Johansson, and L. Tegner, eds., Arkitektikopia, Uppsala (1982).
59. K. Kobashi and R. D. Etters, Lattice dynamics of solid I₂ under high pressure, J. Chem. Phys. 79:3018 (1983).
60. H. K. Koski and E. Sandor, Neutron powder diffraction study of the low-temperature phase of solid acetylene-d₂, Acta. Cryst. B 31:350 (1975); G. J. H. van Nes and F. van Bolhuis, Single-crystal structures and electron density distributions of ethane, ethylene, and acetylene. II. Single-crystal structure determination of acetylene at 141 K, Acta. Cryst. B 35:2580 (1979).
61. R. LeSar, Calculated high-pressure properties of solid acetylene and possible polymerization paths, J. Chem. Phys. 86:1485 (1987).
62. K. Aoki, Y. Kakudate, M. Yoshida, S. Usuba, K. Tanaka, and S. Fujiwara, Raman scattering observations of phase transitions and polymerizations in acetylene at high pressure, Solid State Commun. 64:1329 (1987).
63. K. Aoki, Y. Kakudate, S. Usuba, M. Yoshida, K. Tanaka, and S. Fujiwara, High-pressure Raman study of liquid and crystalline C₂H₂, J. Chem. Phys. (in press); K. Aoki, S. Usuba, M. Yoshida, Y. Kakudate, K. Tanaka, and S. Fujiwara, J. Chem. Phys. (submitted).
64. A. I. Katz, D. Schiferl, and R. L. Mills, New phases and chemical reactions in solid CO under pressure, J. Phys. Chem. 88:3176 (1984).
65. H. B. Radousky, W. J. Nellis, M. Ross, D. C. Hamilton, and A. C. Mitchell, Molecular dissociation and shock-cooling in fluid nitrogen at high densities and temperatures, Phys. Rev. Lett. 57:2419 (1986); W. J. Nellis, N. C. Holmes, A. C. Mitchell, and M. van Thiel, Phys. Rev. Lett. 53:1661 (1984).
66. A. K. McMahan and R. LeSar, Pressure dissociation of solid nitrogen under 1 Mbar, Phys. Rev. Lett. 54:1929 (1985).
67. R. Reichlin, D. Schiferl, S. Martin, C. Vanderborgh, and R. L. Mills, Phys. Rev. Lett. 55:1464 (1985).
68. D. Schiferl and R. LeSar, Raman spectroscopy on simple molecular systems at very high density, this volume.